



OPEN ACCESS

EDITED BY

Fernanda Fidalgo,
University of Porto, Portugal

REVIEWED BY

Suchismita Roy,
University of California, San Diego,
United States
Bruno Sousa,
University of Porto, Portugal

*CORRESPONDENCE

Huiying Liu

✉ hyliuok@aliyun.com

Shengqun Pang

✉ pangshqok@shzu.edu.cn

RECEIVED 07 April 2024

ACCEPTED 31 May 2024

PUBLISHED 17 June 2024

CITATION

Cong Y, Chen X, Xing J, Li X, Pang S and Liu H (2024) Nitric oxide signal is required for glutathione-induced enhancement of photosynthesis in salt-stressed *Solanum lycopersicum* L.
Front. Plant Sci. 15:1413653.
doi: 10.3389/fpls.2024.1413653

COPYRIGHT

© 2024 Cong, Chen, Xing, Li, Pang and Liu.
This is an open-access article distributed under the terms of the [Creative Commons Attribution License \(CC BY\)](https://creativecommons.org/licenses/by/4.0/). The use, distribution or reproduction in other forums is permitted, provided the original author(s) and the copyright owner(s) are credited and that the original publication in this journal is cited, in accordance with accepted academic practice. No use, distribution or reproduction is permitted which does not comply with these terms.

Nitric oxide signal is required for glutathione-induced enhancement of photosynthesis in salt-stressed *Solanum lycopersicum* L

Yundan Cong^{1,2}, Xianjun Chen³, Jiayi Xing^{1,2}, Xuezhen Li^{1,2}, Shengqun Pang^{1,2*} and Huiying Liu^{1,2*}

¹Department of Horticulture, Agricultural College, Shihezi University, Shihezi, Xinjiang, China, ²Key Laboratory of Special Fruits and Vegetables Cultivation Physiology and Germplasm Resources Utilization of Xinjiang Production and Construction Corps, Shihezi, Xinjiang, China, ³School of Life and Health Science, Kaili University, Kaili, Guizhou, China

Reduced glutathione (γ -glutamyl-cysteinyl-glycine, GSH), the primary non-protein sulfhydryl group in organisms, plays a pivotal role in the plant salt stress response. This study aimed to explore the impact of GSH on the photosynthetic apparatus, and carbon assimilation in tomato plants under salt stress, and then investigate the role of nitric oxide (NO) in this process. The investigation involved foliar application of 5 mM GSH, 0.1% (w/v) hemoglobin (Hb, a nitric oxide scavenger), and GSH+Hb on the endogenous NO levels, rapid chlorophyll fluorescence, enzyme activities, and gene expression related to the Calvin cycle in tomato seedlings (*Solanum lycopersicum* L. cv. 'Zhongshu No. 4') subjected short-term salt stress (100 mM NaCl) for 24, 48 and 72 hours. GSH treatment notably boosted nitrate reductase (NR) and NO synthase (NOS) activities, elevating endogenous NO signaling in salt-stressed tomato seedling leaves. It also mitigated chlorophyll fluorescence (OJIP) curve distortion and damage to the oxygen-evolving complex (OEC) induced by salt stress. Furthermore, GSH improved photosystem II (PSII) electron transfer efficiency, reduced Q_A^- accumulation, and countered salt stress effects on photosystem I (PSI) redox properties, enhancing the light energy absorption index (PI_{abs}). Additionally, GSH enhanced key enzyme activities in the Calvin cycle and upregulated their genes. Exogenous GSH optimized PSII energy utilization via endogenous NO, safeguarded the photosynthetic reaction center, improved photochemical and energy efficiency, and boosted carbon assimilation, ultimately enhancing net photosynthetic efficiency (P_n) in salt-stressed tomato seedling leaves. Conversely, Hb hindered P_n reduction and NO signaling under salt stress and weakened the positive effects of GSH on NO levels, photosynthetic apparatus, and carbon assimilation in tomato plants. Thus, the positive regulation of photosynthesis in tomato seedlings under salt stress by GSH requires the involvement of NO.

KEYWORDS

Calvin cycle, fast OJIP fluorescence rise, glutathione, nitric oxide, salt stress, tomato

1 Introduction

China is the world's largest horticultural country, Nevertheless, the escalation of secondary soil salinization, attributed to issues like high cropping intensity, excessive fertilization, and unique water transport mechanisms during production, poses a significant hurdle to the development and productivity of greenhouse crops in China (Zhu, 2016). Plant growth and development are closely linked to their photosynthesis, which is very sensitive to salt stress (Yang et al., 2022). Under salt stress, the photochemical efficiency of the plant photosystem is reduced, leading to overexcitation of the light-trapping antennae and the generation of oxidative stress. Sustaining photosynthesis under salt stress conditions hinges on regulating the photosynthetic apparatus. Moreover, salt stress induces photochemical bursts and diminishes photosynthetic quantum efficiency (Zushi and Matsuzoe, 2017), salt stress can also limit photosynthesis in plants by inactivating CO₂ assimilating enzymes (Li et al., 2022a), resulting in reduced products of photosynthetic carbon assimilation and, in severe instances, potential plant death (Fatma et al., 2014). Tomato (*Solanum lycopersicum* L.) is a significant vegetable crop in horticulture, exhibiting moderate salt tolerance but some sensitivity to salt stress (Xu et al., 2023). Hence, exploring the photosynthetic acclimation mechanism of tomatoes under salt stress is valuable for improving their salt tolerance, reducing the damage caused by salt stress, breeding a resilient crop. Rapid chlorophyll fluorescence-induced kinetic analysis (JIP-test) is an analytical method established on the basis of biofilm energy flow. The JIP-test allows for rapid diagnosis of damage to the structure of the photosynthetic apparatus of a plant before it develops a visible pheno (Baker, 2008; Timilsina et al., 2022).

Reduced glutathione (γ -glutamyl-cysteinyl-glycine, GSH), a redox-active molecule, plays a pivotal role in the plant stress responses through redox pairs (GSH/GSSG) in the ascorbate-glutathione (AsA-GSH) cycle (Yao et al., 2021), glutathione, thioredoxin system, and other pathways. GSH can enhance the ability of plants to cope with challenges by protecting photosystem II by reducing reactive oxygen species (ROS) production (Zhou et al., 2018), protecting photosystem components, and increasing net photosynthetic rate (Mueller-Schuessele et al., 2020). Additionally, GSH collaborates with melatonin (Goodarzi et al., 2020), ascorbic acid, proline, or redox molecules (Semida et al., 2021) to collectively engage in stress-induced signaling pathways.

Nitric oxide (NO), a crucial bioactive plant molecule, regulates plant defense responses to various negative stressors. NO can effectively alleviate chlorophyll degradation, damage to the photosynthetic apparatus, reduced photochemical activity, and light energy conversion efficiency of PSII under stress, this enhances the plants' photosynthetic adaptation (Murchie and Niyogi, 2011; Zhou et al., 2018). To date, more studies have been reported on the involvement of GSH in NO-controlled mitigation of adversity stress (Gautam et al., 2021; Wu et al., 2021; Xu et al., 2023). S-nitrosoglutathione (GSNO), a NO transporter and donor in plants, acts as a link between ROS and reactive nitrogen (RNS) signaling pathways, playing an important role in various plant signaling and defense reactions (Khan et al., 2023). GSNO/NO

regulates the antioxidant system in different abiotic stress environments and improves plant resistance, suggesting that GSH participates in the NO signaling pathway to combat abiotic stresses (Hasan et al., 2016). The previous study demonstrated a synergistic role of NO and GSH in enhancing PSII activity and PSI transduction in cucumber leaves exposed to low-temperature stress (Yang et al., 2023). Currently, only a few studies have reported NO contributions to reducing abiotic stress-induced damage in plants via GSH (Hasan et al., 2016). Alamri et al. (2021) reported that GSH mitigation of arsenic toxicity in *Solanum melongena* requires the involvement of endogenous NO.

The authors' previous studies demonstrated that exogenous GSH protects the photosynthetic apparatus from oxidative damage, increases PSII efficiency, and balances the uneven distribution of light energy by maintaining chloroplast redox balance and increasing ROS absorption capacity. GSH therefore effectively mitigates the inhibitory effects of salt on the growth and photosynthesis of tomato seedlings (Zhou et al., 2018). Furthermore, in another of the authors' studies, the application of the NO scavenger Hb (hemoglobin bovine) reduced the exogenous GSH role in inducing endogenous NO production and increasing the antioxidant capacity of tomato (Wen et al., 2018). NO involvement was therefore hypothesized in the modulation of salt acclimatization by exogenous GSH. However, the role of exogenous GSH in regulating the structure and function of the photosynthetic and carbon assimilation systems in tomatoes under salinity stress, as well as the potential involvement of NO in the photoadaptive mechanism by which GSH alleviates salt stress, is still unclear. Therefore, the present study investigated the role of GSH in photosynthetic efficiency, the kinetic properties of rapid chlorophyll fluorescence induction, and carbon assimilation capacity in salt-stressed tomato seedlings via exogenous application of GSH, Hb, and Hb + GSH. NO involvement in the photosynthetic acclimatization induced by GSH was then detected and elucidated.

2 Materials and methods

2.1 Growing conditions and treatments

The hydroponics experiment was conducted in a greenhouse at Shihezi University, Xinjiang Uygur Autonomous Region, China. Tomato seeds (*Solanum lycopersicum* L. cv. 'Zhongshu No. 4') obtained from Shihezi Yaxin Seeds, China, Soak tomato seeds in warm water at 65°C for 30 minutes, stirring constantly during this time to allow them to fully soak. Subsequently, the seeds were gently rinsed with deionized water and planted in a 2:1 (v/v) charcoal and vermiculite mixture. The seedlings were grown under ambient conditions of 20–26°C, 40–60% relative humidity (RH) and approximately 500 $\mu\text{mol}\cdot\text{photons}\cdot\text{m}^{-2}\cdot\text{s}^{-1}$ light intensity at noon. Upon reaching three fully mature leaves, uniform and healthy tomato seedlings were selected, roots were cleaned, and then transferred to a hydroponic system with a foam lid. The system was filled with 10 L of Hoagland's nutrient solution (pH 6.2) prepared using demineralized water.

After allowing tomato seedlings to pre-culture for 7 days, five treatments were employed in the study (Table 1). The NaCl was added to the Hoagland nutrient solution, and GSH and Hb were sprayed on the leaves at 10:00 a.m every day. The concentrations of NaCl, GSH and Hb were established based on the pre-test results (Zhou et al., 2017; Wen et al., 2018). The research adopted a randomized block design with three replicates. Fully expanded functional young tomato seedling leaves in the third down from the growth point were chosen and sampled (with veins removed) at 24, 48, 72 hours post-treatment. The harvested leaves were rapidly frozen in liquid nitrogen and stored at -80°C for subsequent enzyme activity and gene expression assessments.

2.2 Visualization and quantification of endogenous NO signal

After 24, 48 and 72 hours of treatment, tomato leaves were sectioned into 5 x 5 mm² pieces a dark-incubated in Tris-HCl buffer (10 mM Tris, containing 10 μM DAF-2DA, pH 7.4) for 30 min at 25°C. The excitation and emission wavelengths were 495 and 515 nm, correspondingly. Rinse 2–3 times with fluorescent dye-free buffer to remove excess fluorescent probe. Samples were examined utilizing a ZEISS LSM 510 META laser confocal scanning microscope (Zeiss, Germany). The mean fluorescence intensity of each field of view was quantified using the LSM510 software supplied with the instrument (Li et al., 2022a).

2.3 Assessment of nitrate reductase and NO Synthase activities

NR and NOS activities in tomato seedling leaves were measured using specific kits (Nanjing JianCheng Bio, China).

2.4 Determination of photosynthetic gas exchange parameters

Functional tomato leaves were harvested 24, 48, 72 hours post-treatment. Photosynthetic parameters were assessed with the CIRAS-3 photosynthesis system (PP Systems, USA) (Diao et al., 2014).

TABLE 1 Experimental protocols employed to investigate the impact of salt stress on tomato seedlings.

Treatment	Control	NaCl	NaCl +GSH	NaCl +Hb	NaCl +Hb +GSH
NaCl	0 mM	100 mM	100 mM	100 mM	100 mM
GSH	—	—	5 mM	—	5 mM
Hb	—	—	—	0.1% (W/V)	0.1% (W/V)

100 mM NaCl is added to the Hoagland nutrient solution. Hb, GSH Spray on the leaves.

2.5 Polyphasic fluorescence transients and JIP-test parameters

Chlorophyll-a fluorescence kinetics (OJIP curves) and modulated reflectance kinetics at 820 nm (I/I₀ curves) were measured in tomato plants under various treatments using a multifunctional plant efficiency analyzer (Hansatech Instrument Ltd, Lynn, UK). After a two-hour dark acclimatization period, the leaves were exposed to saturating pulsed light (3,000 μmol photons m⁻² s⁻¹). The recorded fluorescence signals ranged from 0.01 ms to 3 S. The average OJIP measurement value of the OJIP measurement was calculated for the leaves (three tomato plants per treatment, n=3) in each treatment, and the fast OJIP curve was plotted. The spider plot data were presented as C_{test}/C_{Control}, where C_{test} and C_{Control} represented the data from the treatment and control groups, respectively. The JIP-test analysis of the OJIP curve provided parameters listed in Table 2.

2.6 Calvin cycle key enzymes

Rubisco activity was measured spectrophotometrically following the method of Lilley and Walker (1974), with some modifications. The total activity was assayed after the crude extract had been activated in a 0.1 ml activation mixture containing 33 mM Tris-HCl (pH 7.5), 0.67 mM EDTA, 33 mM MgCl₂ and 10 mM NaHCO₃ for 15 min. Initial Rubisco activity measurements were carried out in 0.1 ml of reaction medium containing 5 mM HEPES-NaOH (pH 8.0), 1 mM NaHCO₃, 2 mM MgCl₂, 0.25 mM dithiothreitol (DTT), 0.1 mM EDTA, 1 U of glyceraldehyde 3-phosphate dehydrogenase, 0.5 mM ATP, 0.015 mM NADH₂, 0.5 mM phosphocreatine, 0.06 mM ribulose-1,5-bisphosphate (RuBP), and 10 μl of extract. The change in absorbance at 340 nm was monitored for 90 s (YuPing et al., 2012). Activities of RCA, PGK, GAPDH, FBPase, and TK were measured using specific biochemical spectrophotometric kits (Yuchun Bio, China). SBPase activity was determined following the method of Harrison et al. (1998) method. FBA activity was measured using biochemical kits (COMIN Bio, China).

2.7 Quantitative real-time PCR

The total RNA was extracted from tomato leaves using the Trizol method. Primers used in this study were designed with Primer 6.0 based on the NCBI database (Supplementary Table 2). The tomato *actin* gene served as an internal control (Li et al., 2022a; Zhang et al., 2023). All primers were synthesized by Biotech Bioengineering Co. (Shanghai, China).

High-purity and integrity total RNA was reverse transcribed into cDNA using the Hyper Script™ III RT SuperMix for qPCR with gDNA Remover (NovaBio, China) following the manufacturer's instructions. qRT-PCR amplification was conducted using the 2 x S6 Universal SYBR qPCR Mix (NovaBio, China). Real-time PCR was performed using a CFX96™ Real-Time PCR System (BIO-RAD, America), following the methods in the

TABLE 2 Summary of parameters and formulae using data extracted from JIP-test.

Parameters	Explanation
$PI_{ABS=RC/ABS}$ [$\phi P_o/(1-\phi P_o)$] [$\psi_o/(1-\psi_o)$]	Performance index on absorption basis
$S_m = (Area)/(F_m - F_o)$	Normalized total complementary area
$ABS/RC=M_o(1/V_j)$ ($1/\phi P_o$)	Average absorbed photon flux per PSII reaction center
$ET_o/RC =M_o(1/V_j)$ ($1/V_j$)	Electron transport flux per RC (at $t=F_o$)
$DI_o/RC =ABS/RC - TR_o/RC$	Dissipated energy flux per RC (at $t=F_o$)
$\phi P_o=TR_o/ABS = [1 - (F_o/F_m)]$	Maximum quantum yield of primary photochemistry
$\phi D_o=1-\phi P_o = (F_o/F_m)$	Quantum yield at $t=F_o$ for energy dissipation
$\phi E_o=ET_o/ABS = [1 - (F_o/F_m)] \psi_o$	Quantum yield for electron transport (at $t=F_o$)
$\Psi_o=ET_o/TR_o = (1-V_j)$	Probability that a trapped exciton moves an electron into the electron transport chain beyond Q_A^- (at $t=F_o$)
$ABS/CS_m = F_m$	Absorbed photon flux per cross section
$TR_o/CS_m =\phi P_o$ (ABS/CS_m)	Maximum trapped exciton flux per cross section
$ET_o/CS_m =\phi E_o$ (ABS/CS_m)	Electron transport flux from Q_A to Q_B per cross section
$DI_o/CS_m = (ABS/CS_m) - (TR_o/CS_m)$	Dissipated energy flux per RC (at $t=F_m$)
$RC/CS_m = \phi P_o$ (V_j/M_o) (ABS/CS_m)	Probability that PSII Chl functions as an active center
$\delta R_o = RE_o/ET_o = (1 - V_j)/(1 - V_j)$	Efficiency of electron movement from the reduced intersystem electron acceptors to the PSI end acceptors
$\phi R_o = RE_o/ABS = TR_o/ABS (1 - V_j)$	Quantum yield for reduction of end electron acceptors at the PSI acceptor side

ChamQ Blue Universal SYBR qPCR Master Mix (Vazyme Biotech Co., Ltd, Nanjing, China). Three parallel replicates were prepared for each sample stored at -80°C , and biological replicates were performed for each gene. The $2^{-\Delta\Delta Ct}$ method Livak and Schmittgen (2001) was used to calculate the relative gene expression.

2.8 Statistical analysis

Data were analyzed using IBM SPSS 25 statistical software with one-way ANOVA. Differences' significance was assessed using the Duncan test ($P < 0.05$). Graphs were created using OriginPro 2023. Values in tables and graphs represent the mean \pm standard deviation (SD). Three parallel replicates were prepared for each sample.

3 Results

3.1 Endogenous NO accumulation in tomato leaves under different treatments

As shown in Figure 1, in comparison with Control, the average NO fluorescence intensity, NR and NOS activity during the three measurement periods of NaCl treatment were significantly reduced by 41.3–42.7%, 59.1–69.9%, and 43.5–54.3%, respectively. Conversely, treatment with NaCl+GSH led to a significant increase in NO content, NR and NOS activity by 15.62–39.42%, 51.8–121.4% and 7.6–44.1%, respectively, compared to NaCl treatment. Treatment with NaCl+Hb resulted in a significant decrease in NO content and NR activity at 48 and 72 hours, as well as NOS activity at 72 hours. On the other hand, NaCl+Hb +GSH treatment significantly enhanced NO content, NR and NOS activity throughout the treatment period compared to NaCl+Hb treatment, with increases of 38.3–49.4%, 21.8–87.3% and 21.2–44.1%, respectively.

3.2 Photosynthetic gas exchange in tomato leaves under different treatments

The application of NaCl significantly reduced the net photosynthetic rate (P_n), stomatal conductance (G_s), intercellular CO_2 concentration (C_i) and transpiration rate (T_r) across all three treatment periods in comparison to Control (Figure 2). Conversely, the NaCl+GSH treatment led to a substantial increase in P_n , C_i , G_s and T_r values throughout the treatment period, showing enhancements 24.3–30.5%, 21.4–32%, 6.0–15.5% and 29.4–41.9%, respectively, when compared to the NaCl treatment. On the other hand, the NaCl+Hb treatment resulted in a notable reduction in P_n , G_s , and T_r throughout the treatment duration, while C_i values experienced at 48 and 72h. In comparison to the NaCl+GSH treatment, P_n , G_s and T_r values over the treatment period, along with C_i at 24 and 72 h, exhibited significant decreases under NaCl +Hb+GSH treatment.

3.3 Impact of various treatments on the kinetic properties of transient fluorescence induction (JIP-test)

3.3.1 OJIP curves

Under NaCl stress, the OJIP curves displayed deformations compared to Control, indicating a reduced amplitude of the I-P phase (Figure 3A-C). The entire curve flattened, and the amplitudes of the I and P phases, as well as the I-P phase of the OJIP curves, gradually decreased with prolonged treatment time. In contrast to the NaCl treatment, the shape of the OJIP curves underwent significant alterations during NaCl+Hb treatment, leading to a notable decrease in the amplitude of the I-P phase. However, the amplitudes of the I, P and I-P phases were significantly heightened

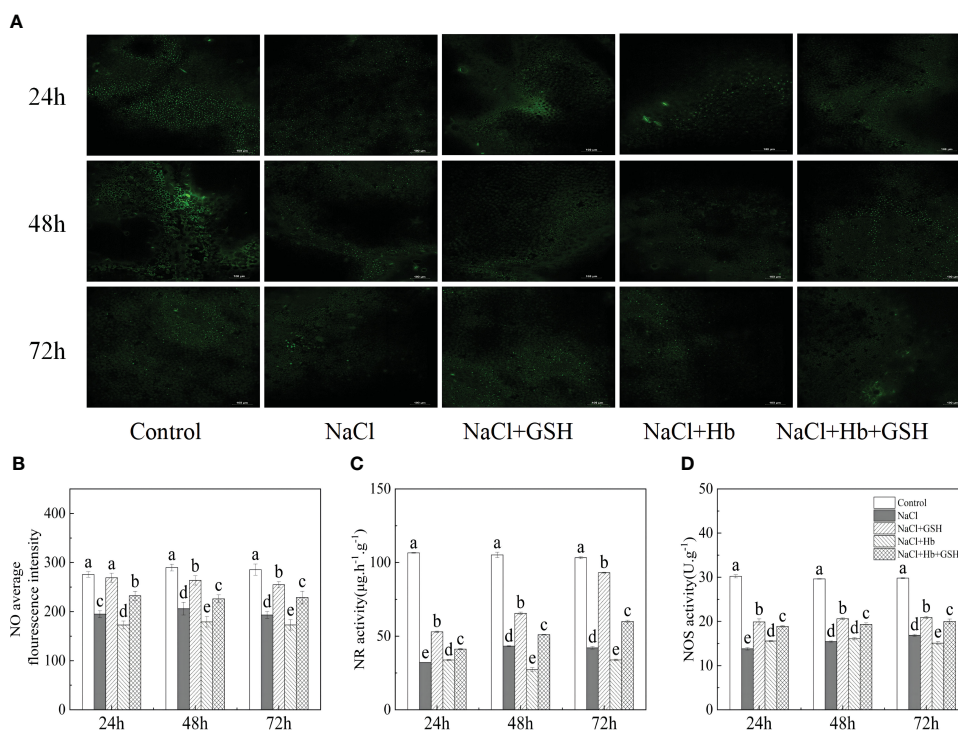


FIGURE 1 Effects of GSH (γ -glutamyl-cysteinyl-glycine), Hb (Hemoglobin, NO scavenger), Hb+GSH on NO fluorescence imaging (A), average fluorescence intensity (B), nitrate reductase (NR) activity (C), and nitric oxide synthase (NOS) activity (D) in leaves of salt-stressed tomato seedlings. Notes: The green spots in figure A are the NO signal, and the short white line in the lower right corner is the 100- μ m scale. Control, no added NaCl and sprayed with distilled water; NaCl, addition of 100 mM NaCl and sprayed distilled water; NaCl+GSH, added 100 mM NaCl, and sprayed 5 mM GSH; NaCl+Hb, with added 5 mM GSH. The results are presented as the mean \pm SD (standard deviation) (n=3). Different lowercase letters represent significant differences, and the same lowercase letters represent no significant differences ($p < 0.05$, Duncan's range test).

throughout the three periods of NaCl+GSH treatment. However, the amplitudes of the I, P and I-P phases were significantly enhanced during the three periods of NaCl + GSH treatment. I-P phase amplitude significantly decreased, while the amplitudes of the I and P phases as well as the I-P phase were significantly higher in the three periods under NaCl+GSH treatment. Furthermore, the amount of phase I and P in OJIP curves treated with NaCl+Hb+GSH was lower than in those treated with NaCl+GSH during the three measurement periods. Normalization of the OJIP curves (Figure 3D-F) demonstrated a significantly higher J phase under NaCl stress compared with the control. This suggested an inhibition of Q_A to Q_B electron transfer on the PSII receptor side and a large accumulation of Q_A^- . Exogenous GSH application reduced the J phase under NaCl stress to varying degrees. The Hb application further increased the J phase under NaCl stress, weakening the effect of GSH. These findings indicate that GSH mitigated the partial damage to the PSII reaction center and decreased the ability of the PSII donor side to transfer electrons downstream under salt stress conditions, independently of NO.

The presence of L and K-bands at 0.15 and 0.3 ms and the rise in ΔW_L and ΔW_K values were recognized as specific markers of vesicle-like dissociation and damage to the PS II donor-side complex (OEC), respectively. ΔW_L at 24 and 72 h and ΔW_K at 48 and 72 h were significantly higher under NaCl treatment compared to the control, while ΔW_L and ΔW_K were significantly lower under NaCl+GSH

treatment compared with NaCl treatment to varying degrees (Figure 4). These results suggested that GSH application attenuates salt stress-induced vesicle dissociation and OEC damage. In addition, the Hb application further enhanced ΔW_L at 48 and 72 h of salt stress treatment and ΔW_K at the three measurement periods. The Hb application also enhanced ΔW_K under NaCl+GSH treatment.

3.3.2 JIP-test parameters

NaCl treatment had a significant impact on tomato plants compared to Control (refer to Figure 5A-C). There was a notable increase in the relative variable fluorescence (V_i) at point I, the relative variable fluorescence (V_j) at point J, the maximum rate at which Q_A was fully reduced (M_o), the quantum ratio used for heat dissipation (ϕD_o) in tomato seedling leaves. Furthermore, this increase was observed in the ratio of exciton-driven electron transfer by excitons captured by the PSII active reaction center (Ψ_o), the quantum efficiency of the electron transfer from Q_A^- to the electron transfer chain (ϕE_o), the photosynthetic performance index (PI_{abs}), the efficiency of electron transfer from Q_B to the PSI receptor side (δR_o), the quantum yield of the terminal electron acceptor on the reduced PSI receptor side (ϕR_o). These findings indicate that NaCl stress resulted in a decrease in the electron transfer capacity on the PSII receptor side and in the activation of the active PSII reaction centers. In contrast, NaCl+Hb treatment further significantly increased M_o and ϕD_o , while significantly decreasing Ψ_o , ϕE_o , PI_{abs} and ϕR_o . GSH application effectively

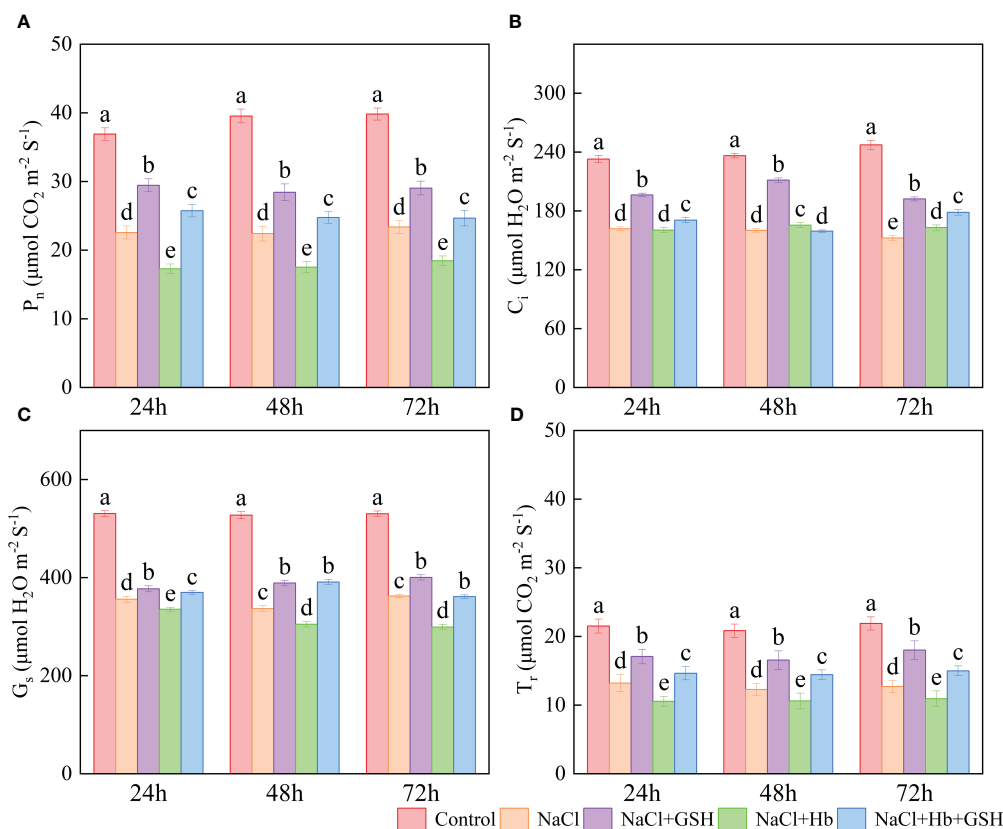


FIGURE 2 Effects of GSH, Hb, and Hb+GSH on the net photosynthetic rate (P_n , **A**), intercellular CO_2 concentration (C_i , **B**), transpiration rate (T_r , **C**), and stomatal conductance (G_s , **D**) in leaves of salt-stressed tomato seedlings. Notes: Control, no added NaCl and sprayed with distilled water; NaCl, addition of 100 mM NaCl and sprayed distilled water; NaCl+GSH, added 100 mM NaCl, and sprayed 5 mM GSH; NaCl+Hb, with added 5 mM GSH. The results are presented as the mean \pm SD (standard deviation) ($n=3$). Different lowercase letters represent significant differences, and the same lowercase letters represent no significant differences ($p < 0.05$, Duncan's range test).

alleviated M_o and ϕD_o increases under NaCl treatment to varying degrees and restored Ψ_o , ϕE_o , PI_{abs} , δR_o and ϕR_o decreases to the control group levels (72 h) with extended treatment time. However, the Hb application weakened the effect of GSH on the above parameters under NaCl stress.

The 820 nm fluorescence reflectance kinetic curve (I/I_o) is used to determine PSI complex activity due to adversity stress (Figure 6A-C), which demonstrated that NaCl stress could severely deform the leaf I/I_o curve compared to the control. This was expressed by the elevation of the lowest point of the descending phase and the decrease of the highest point of the ascending phase, suggesting that the PSI redox capacity was inhibited by salt stress. In contrast, the GSH application restored I/I_o curve deformation under NaCl treatment to varying degrees. The Hb application further heightened I/I_o curve deformation under NaCl stress and weakened the effect of exogenous GSH in alleviating the deformation.

3.3.3 PSII reaction center activity and excited cross section phenomenological energy fluxes

In tomato seedling leaves, the unit activity of the PSII reaction center (RC) showed a significant increase in the energy absorbed and thermally dissipated by RC (ABS/RC and DI_o/RC), along with a notable decrease in the energy transferred by RC (ET_o/RC) under NaCl treatment compared to the Control conditions (Figure 7A-C).

Notably, NaCl+GSH treatment led to a significant increase in ET_o/RC and a decrease in ABS/RC , DI_o/RC and TR_o/RC . Conversely, NaCl+Hb treatment increased ABS/RC , DI_o/RC and TR_o/RC values. Additionally, the ABS/RC , DI_o/RC and TR_o/RC values were significantly reduced in the NaCl+Hb+GSH treatment compared to the NaCl+Hb treatment. For the unit leaf cross-sectional area (CS_m), the number of RCs (RC/CS_m) and the energy absorbed and captured by the CS_m (ABS/CS_m and TR_o/CS_m) were significantly lower in the CS_m under NaCl stress compared to the Control. Although NaCl+GSH treatment significantly increased ABS/CS_m , TR_o/CS_m , ET_o/CS_m and RC/CS_m , both NaCl+Hb and NaCl+Hb+GSH treatments significantly decreased ABS/CS_m , TR_o/CS_m , ET_o/CS_m and RC/CS_m values to varying degrees compared to NaCl and NaCl+GSH treatments (Figure 7A-C). The energy flux model is depicted in Figure 7D, E.

3.4 The role of NO in GSH-induced CO_2 assimilation under salt stress

NaCl treatment significantly reduced Rubisco (both initial and total), RCA, GAPDH, PGK, FBA, FBPase, SBPase and TK activity by 46.7–50.1%, 50.3–54.6%, 11.9–24.9%, 40.6–51.1%, 30.1–35.7%, 29.9–34.5%, 33.3–38.8%, 40.5–49.9% and 40.2–43.8%, respectively

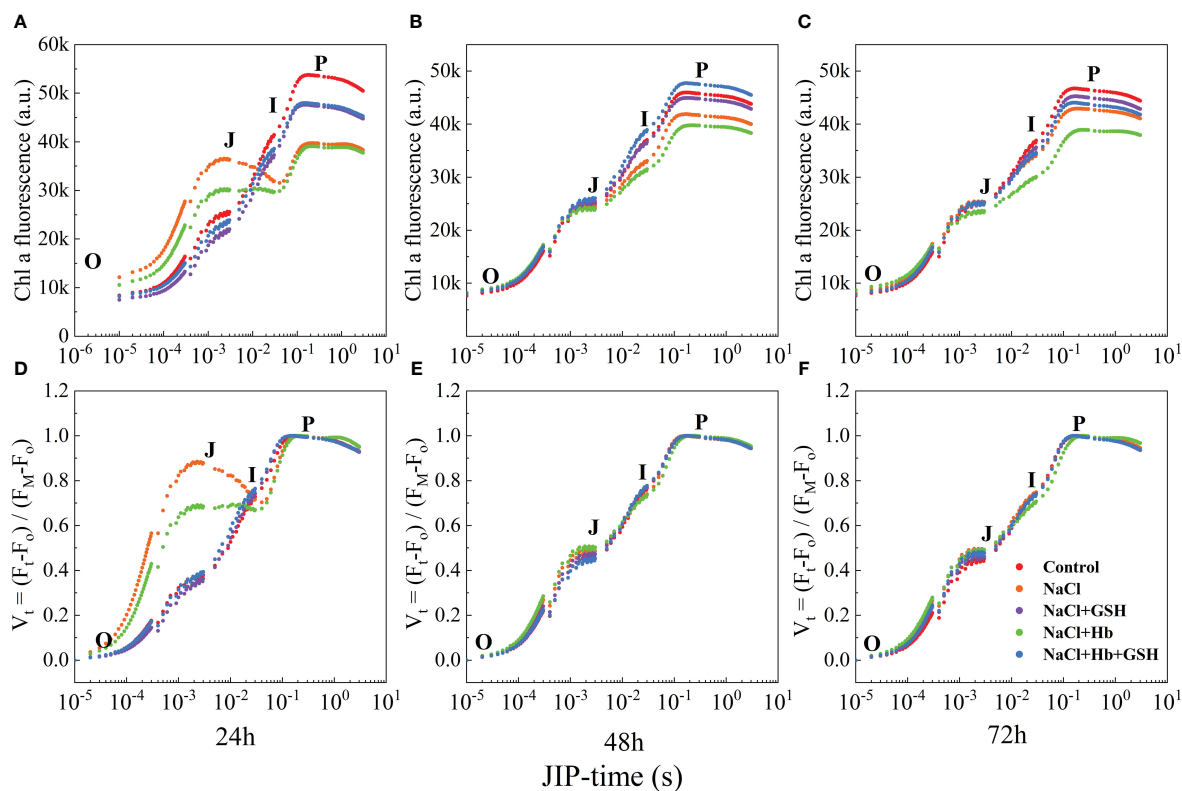


FIGURE 3
The fast chlorophyll a fluorescence induction (OJIP) curves (A–C) and normalized transients between O- and P-step expressed as $V_t = [(F_t - F_o) / (F_M - F_o) - F_o]$ (D–F) in leaves of salt-stressed tomato seedlings as affected by GSH, Hb, and Hb+GSH.

(Figure 8). However, GSH application alleviated the inhibitory effect of NaCl stress, increasing above enzyme activity by 46.1–64.1%, 50.1–73.3%, 8.1–26.0%, 44.1–75.6%, 21.2–42.75%, 32.6–44.5%, 45.1–59.9% 29.1–60.7% and 46.5–62.1%, respectively. NaCl+Hb treatment significantly decreased TK activity, 24-hour RCA activity and 48-hour SBPase activity throughout the treatment period compared to NaCl stress. NaCl+Hb+GSH treatment significantly increased RCA, FBPase, FBA SBPase and TK activity, as well as PGK at 24 and 72 h and GADPH at 48 and 72 h compared to the NaCl+Hb treatment.

The transcript levels of key enzymes involved in CO₂ carboxylation and reduction (*RbcS*, *RbcL*, *RCA*, *PGK* and *GADPH*) and enzymes related to RuBP regeneration (*SBPase*, *FBA*, *FBPase* and *TK*) were significantly downregulated under NaCl stress (Figure 9). However, NaCl+GSH treatment resulted in a significant upregulation of these genes. Conversely, NaCl+Hb treatment led to a significant downregulation of *FBA* at 24 h, *SBPase* at 48 h, *RbcL* and *PGK* at 72 h, *RbcS* and *RCA* at 24 and 72 h. No significant effects were detected on *GADPH*, *FBPase*, *TK* transcript levels.

4 Discussion

Plant photosynthesis is essential for energy production and metabolism, and is highly susceptible to external environmental

factors (Bahmani et al., 2019). P_n serves as a vital indicator of plant photosynthetic capacity (Simkin et al., 2019). During salt stress, the decrease in P_n can be attributed to both stomatal and non-stomatal limiting factors. In this investigation, the decline in P_n under salt stress coincided with reductions in C_i , G_s , T_r (Figure 2) and PI_{abs} (Figure 5). PI_{abs} is a comprehensive index that reflects photochemical efficiency. Previous studies have indicated that the reduction in PI_{abs} is more sensitive than F_v/F_m , accurately indicating the impairment of the plant's photosynthetic machinery and the decrease in photochemical efficiency under adverse condition (Chen et al., 2021; Li et al., 2022b). The decrease in P_n due to NaCl stress was influenced by both stomatal-limiting and non-stomatal-limiting factors. These results were similar to the studies of *Hordeum jubatum* (Shi et al., 2021) and *Cucumis melo* (Sarabi et al., 2019). Furthermore, a correlation was noted between the reduction in P_n under salt stress and a decrease in NO signaling intensity, along with reduced NOS and NR activity. Conversely, the application of GSH under salt stress led to an improvement in P_n , C_i , G_s and PI_{abs} , accompanied by an increase in NO levels as well as NR and NOS enzyme activity (Figure 2).

NO is widely distributed in various tissues and organs of plants, and exerts a positive regulatory role in plant growth and stress resilience. It is involved in the regulation of diverse physiological processes in plants (Fancy et al., 2017). Its cellular concentrations are decisive for its function, as a signaling molecule at lower

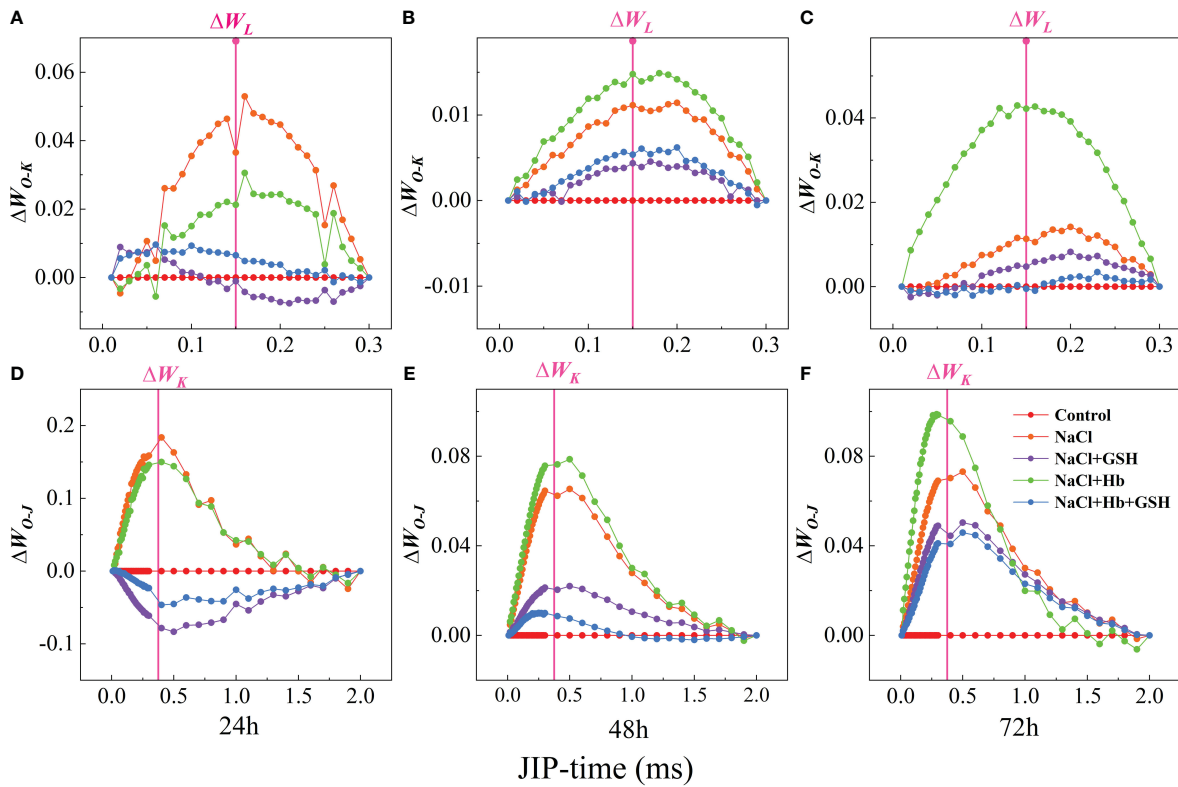


FIGURE 4
 Difference kinetics $\Delta W_{O-K} = W_{O-K(stress)} - W_{O-K(control)}$ (A–C) in a linear time scale from 0 to 300 μs and $\Delta W_{O-J} = W_{O-J(stress)} - W_{O-J(control)}$ (D–F) in a linear time scale from 0 to 2 ms in leaves of salt-stressed tomato seedlings as affected by GSH, Hb, and Hb+GSH. $\Delta W_{O-K} = W_{O-K(stress)} - W_{O-K(control)}$ (A–C), $\Delta W_{O-J} = W_{O-J(stress)} - W_{O-J(control)}$ (D–F).

concentrations, but triggers nitro-oxidative stress and cellular damage when produced at higher concentrations (Wani et al., 2021; Nishat Timilsina et al., 2022; Parveen et al., 2023). Salt stress-induced fluctuations in NO levels have been documented in different plant species, potentially influenced by salt type, stress intensity, duration and plant species. The results showed that external GSH improved P_n in salt-stressed tomato leaves by promoting the production of endogenous NO (Figures 1, 2). To explore if external GSH influenced the photosynthetic capacity of tomato seedlings under salt stress through modulating endogenous

NO levels, we treated tomato seedlings under salt stress with exogenous Hb, a NO scavenger. Numerous studies have previously demonstrated the ability of external Hb to efficiently decrease endogenous NO levels in plants (Shao et al., 2010; Lee and Hwang, 2015; Bahmani et al., 2019; Hu et al., 2023). In this investigation, the application of Hb not only resulted in a further reduction in P_n and endogenous NO levels under salt stress but also attenuated the beneficial impacts of GSH treatment, including the rise in P_n and endogenous NO levels. These findings strongly suggest that GSH mitigates the effects of NaCl stress by mediating

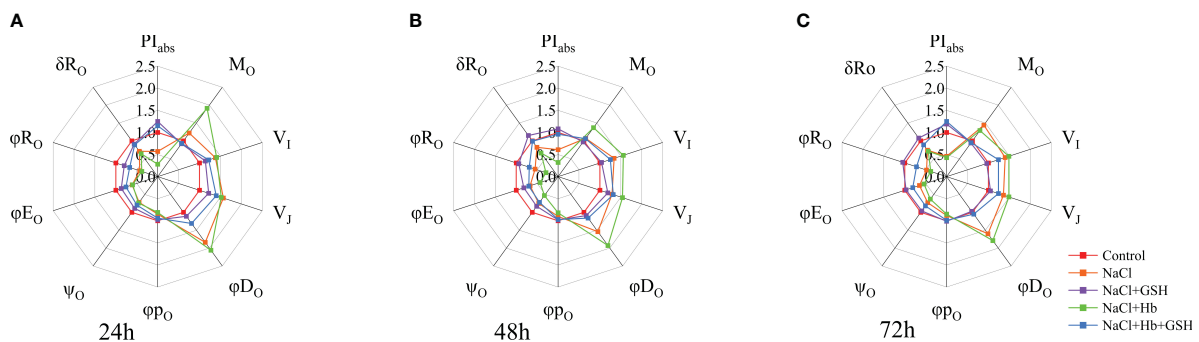


FIGURE 5
 Spider plots were used to assess GSH, Hb, and Hb+GSH treatment influence on JIP-test parameters derived from chlorophyll a fluorescence OJIP transient curves (A–C) in salt-stressed tomato seedling leaves.

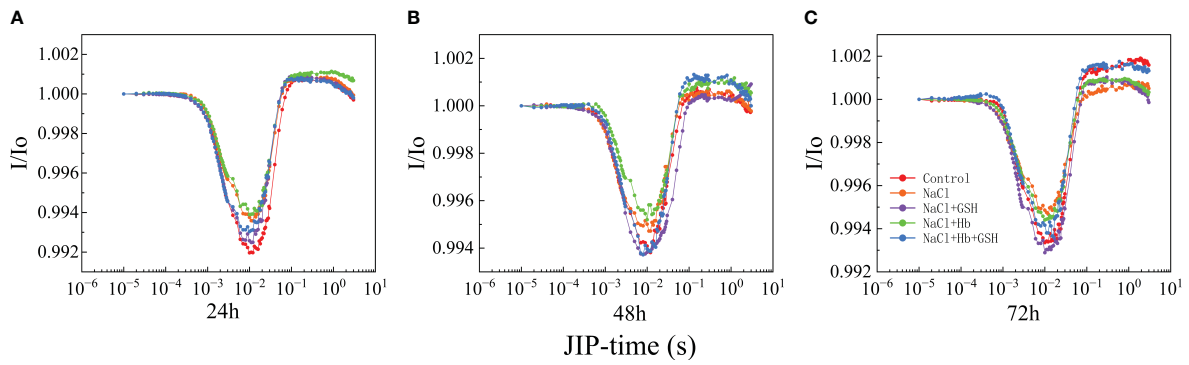


FIGURE 6 Curves of light-induced modulated 820 nm reflection kinetics (I/I_0) (A–C) in leaves of salt-stressed tomato seedlings as affected by GSH, Hb, and Hb+GSH.

endogenous NO levels, and is involved in regulating the decline of P_n in tomato plants. Hb application significantly reduced NR activity at 48 and 72 h and NOS activity at 72 h under salt stress to varying degrees, as well as NR and NOS activity under NaCl +GSH treatment. These results, similar to (Shao et al., 2010), suggested that Hb application also reduced endogenous NO levels via a down-regulation of the NO synthesis pathway.

Salt stress can significantly affect the photosynthetic apparatus, specifically the PSII located in the thylakoid lamellae, PSII is highly vulnerable to salt stress-induced photoinhibition, which can damage the overall photosynthetic efficiency (Zushi and Matsuzoe, 2017). The OJIP curve provides insights into PSII primary photochemical reactions, revealing the impact of

environmental conditions on the photosynthetic apparatus, including the PSII donor and acceptor sides. The J-phase represented Q_A^- rapid accumulation and increased J-phase fluorescence demonstrated a blockage in electron transfer from Q_A to Q_B on the PSII acceptor side. OJIP curve analysis provided insights into PSII functional status and environmental influence. The appearance of the K-band ($\Delta W_K > 0$) before the OJIP curve rising to the J-phase reflected OEC damage on the PSII donor side. The appearance of the L-band with $\Delta W_L > 0$. On the other hand, indicated the dissociation of the basal vesicle-like bodies, resulting in an increased dissociation between the PSII complexes. V_j and V_i reflect the number of reaction centers in the J-phase and I-phase closure, respectively. An increase in V_j was a specific marker of

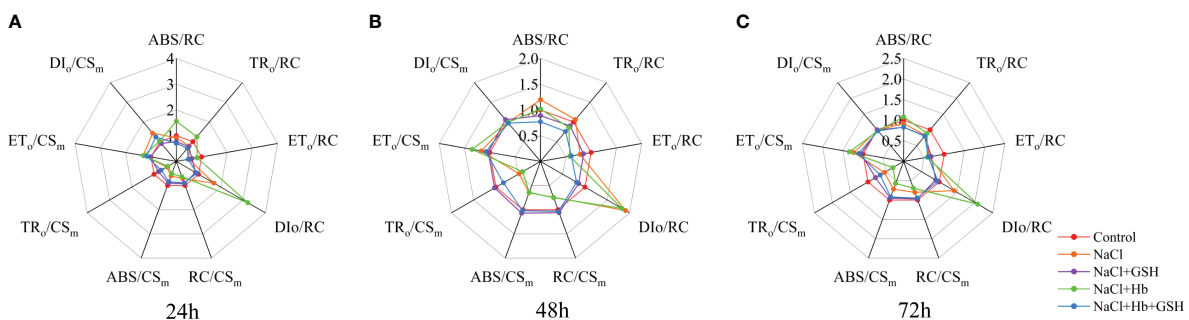
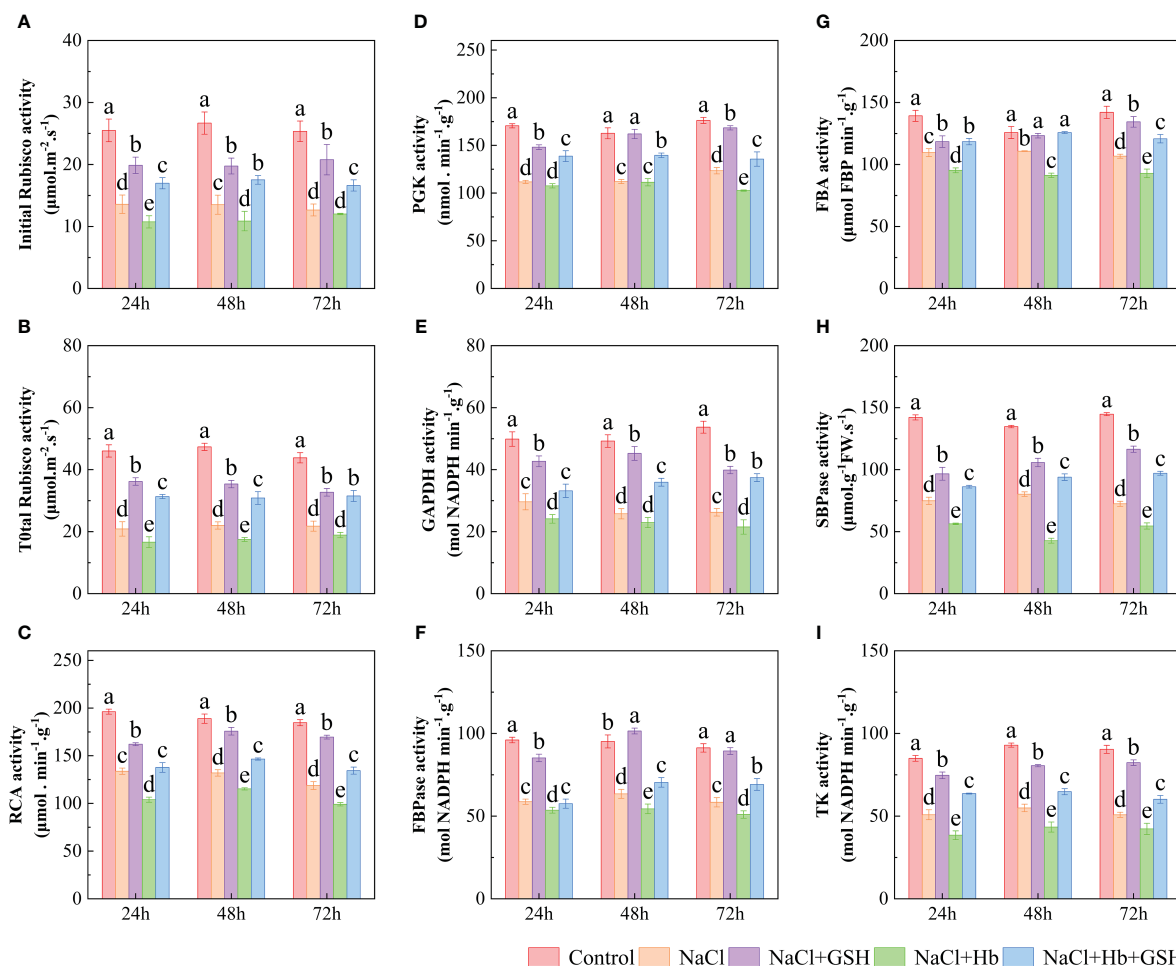


FIGURE 7 Spider plots of the energy distribution parameters per PSII reaction center (RC) and exciting cross-sectional area (CS_m) (A–C) and the energy pipeline model of specific fluxes per RC (D) and phenomenological fluxes per excited CS_m (E) in salt-stressed tomato seedlings as affected by GSH, Hb, and Hb+GSH.



blocked electron transfer from the PSII receptor side Q_A to the secondary quinone receptor Q_B . However, an increase in V_I indicated a decrease in the ability of the PQ pool to accept electrons. In the current study, salt stress reduced the amplitude of the I-P phase and increased the ΔW_K , ΔW_L , and J phases (Figures 3, 4), as well as elevated V_I and V_I values in tomato leaves (Figure 5). These changes indicated that salt stress damaged the PSII donor side OEC and increased dispersion between PSII complexes. This also led to the accumulation of Q_A^- on the PSII acceptor side, resulting in the partial closure of PSII reaction centers. Furthermore, salt stress reduced Ψ_o and ϕE_o while promoting an increase in M_o (Figure 5). These results demonstrated a reduction in the openness of active PSII reaction centers and PQ pool capacity, as well as a decline in electron transfer ability from Q_A on the PSII acceptor side. GSH treatment however protected the PSII donor side OEC and reaction center structure under salt stress and also enhanced electron transfer and photochemical efficiency on the PSII acceptor side (Figures 3, 5).

Conversely, the application of GSH shielded both the OEC and the reaction center structure on the donor side of PSII from salt stress, enhancing electron transfer and the photochemical efficiency of the PSII acceptor side (Figures 3, 5). Furthermore, the use of Hb diminished the favorable outcomes of external GSH on electron transfer at the PSII donor side, the photosynthetic apparatus, and PSII acceptor measurements in NaCl-stressed tomato seedlings. Collectively, these findings indicate that NO is involved in mediating the advantageous effects of GSH on the structure and functionality of the PSII photosynthetic apparatus.

Under normal conditions, the PSII reaction center efficiently converts captured light energy into excitation energy. This energy is primarily utilized for carbon assimilation, while any surplus energy is dissipated as heat. However, under adversity stress, PSII reaction centers become temporarily inactive. Despite the continued absorption of light energy, PSII reaction centers fail to transfer it to the electron transport chain (Murchie and Niyogi, 2011). Additionally, the research illustrated a notable decline in RC/CS_m ,

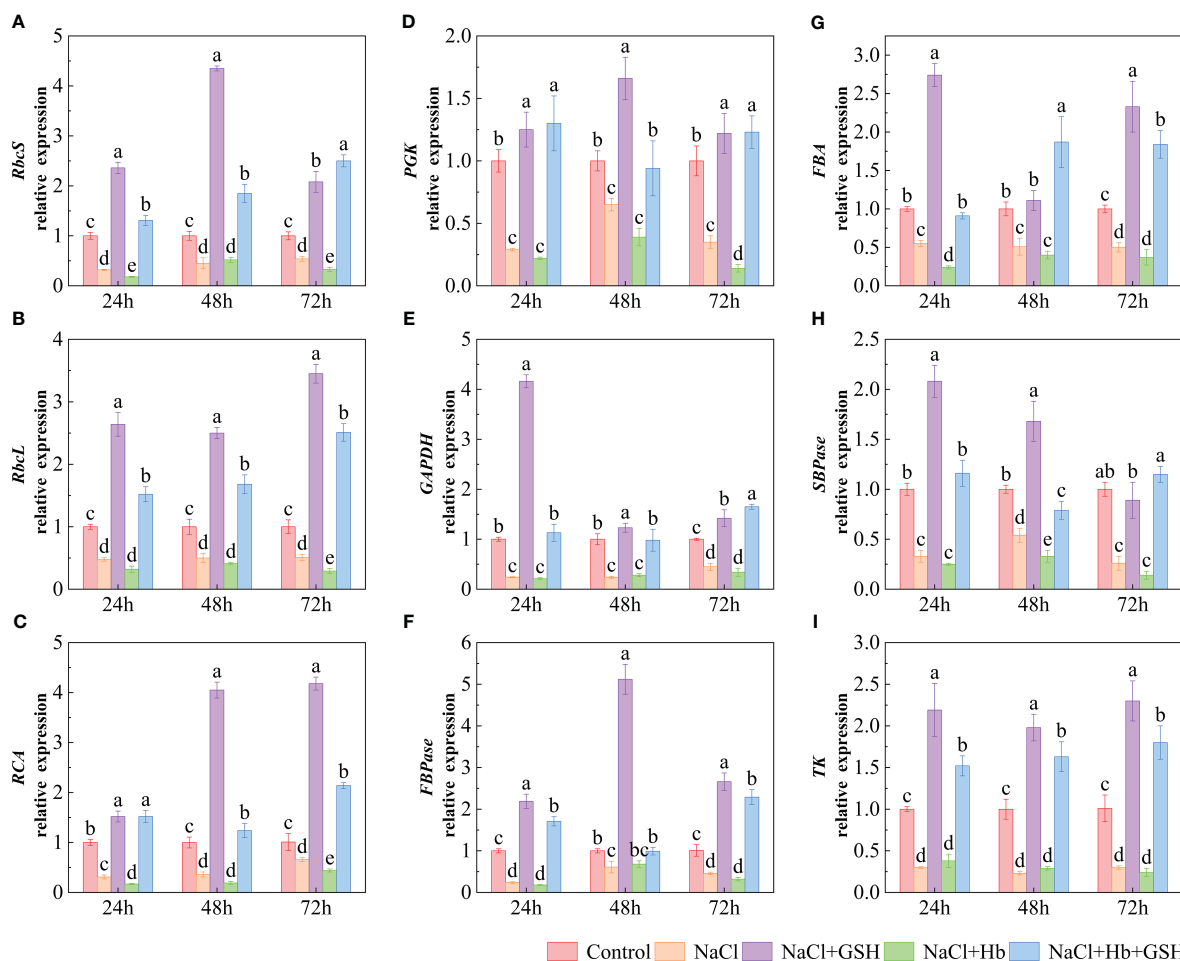


FIGURE 9

The relative expression of genes involved in the Calvin cycle in tomato seedling leaves under salt stress were analyzed for their response to GSH, Hb, and Hb+GSH. *RbcS*, *RbcL*, *RCA*, *PGK*, *GAPDH*, *FBpase*, *FBA*, *SBpase* and *TK* (A-I). Transcript levels were quantified using quantitative PCR, which were then normalized to *actin* expression. Notes: Control, no added NaCl and sprayed with distilled water; NaCl, addition of 100 mM NaCl and sprayed distilled water; NaCl+GSH, added 100 mM NaCl, and sprayed 5 mM GSH; NaCl+Hb, with added 5 mM GSH. The results are presented as the mean \pm SD (standard deviation) (n=3). Different lowercase letters represent significant differences, and the same lowercase letters represent no significant differences (p < 0.05, Duncan's range test).

TR_o/CS_m and ET_o/CS_m in tomato leaves (Figure 7), indicating the degradation or deactivation of reaction centers and a reduction in light energy available for electron trapping and transfer (Li et al., 2017). The decrease in ABS/CS_m and the rise in DI_o/CS_m under salt stress (Figure 7) indicated the activation of defense mechanisms in salt-stressed tomato plants, aligning with the observations of Yuan et al. (2014) findings. On the one hand, mitigating the overaccumulation of light energy by reducing the light energy absorption of PSII antenna pigments, and on the other hand, diminishing the buildup of excess excitation energy through the enhancement of the heat dissipation pathway. Moreover, salt stress induced an elevation in ABS/RC, TR_o/RC and DI_o/RC, while a decrease in RC/CS_m prompted a compensatory reaction. The remaining active RCs exhibited enhanced efficiency in absorbing, converting, and dissipating light energy, leading to improved consumption of excess energy in the electron transport chain (Chen et al., 2021). In contrast, GSH treatment not only mitigated the decrease in ABS/CS_m, TR_o/CS_m and ET_o/CS_m in tomato leaves under salt stress, but also sustained elevated levels

of DI_o/CS_m, ABS/RC, TR_o/RC and DI_o/RC (Figure 7). This protective mechanism optimizes energy allocation in PSII, preventing over-reduction of the photosynthetic electron transport chain and safeguarding the integrity and functionality of both the electron transport chain and the PSII reaction center.

In addition to plant leaf PSII, PSI reaction centers are vulnerable to adversity stress. The I/I_o curves reflect PSI primary photochemical reactions (Yuan et al., 2014). The fast descend phase in the I/I_o curves represents the oxidation of P₇₀₀ and PC, the nadir point is the turning point of the redox of PSI. When the electrons from PSII promote PSI reduction, the I/I_o curve turns to a slow-rising phase, which represents the re-reduction of P₇₀₀ and PC (corresponding to the I-P phase of the OJIP curve) (Guo et al., 2020). Therefore, the I/I_o curve is simultaneously affected by PSI and PSII activity and can reflect the coordination between these photosystems. The decrease in PSI activity prevents the PSII from transferring electrons to PSI, exacerbating the degree of PSII injury, meanwhile, PSI stability can ensure the rapid repair of damaged PSII (Yuan et al., 2014). The results of this study indicated that

exogenous GSH effectively alleviated the reduction of PSI redox capacity in tomato plants under salt stress (Figure 6). Combined with the significant ϕR_0 increase under NaCl+GSH treatment compared with NaCl treatment, it was hypothesized that GSH may enhance PSI activity via an increased ability or amount of electron transfer from PQ to P_{700}^+ , facilitating PSI receptor-side electron transfer and coordinating the connectivity between PSII and PSI. However, the positive GSH effect on PSI in salt-stressed tomato leaves may be weakened by exogenous Hb application (Figures 5, 6). This suggested that PSI activity regulation in salt-stressed tomato leaves by GSH required NO participation.

The Calvin-Benson cycle (CBC) is the primary CO_2 fixation pathway utilized by C3 plants (Jensen et al., 2017). The CBC consists of the following three stages: CO_2 fixation, CO_2 reduction, and RuBP regeneration. Under adversity stress, the maintenance of high photosynthetic carbon assimilation capacity is a prerequisite for high yields (Zhao et al., 2021). Rubisco is the rate-limiting enzyme in CBC which plays a vital role in catalyzing CO_2 fixation. The activity and expression of Rubisco directly influence the efficiency of CO_2 carboxylation and the flow of electrons in the photosynthetic electron transfer chain (Sudhani and Moreno, 2015). *RbcL*, *RbcS*, and *RCA* genes encode the large subunit, small subunit and ribulose-1,5-bisphosphate carboxylase, respectively, which work closely together to regulate the structure and function of Rubisco holoenzymes. Many studies have reported that abiotic stresses (including low light, low temperature, drought, and other stresses) can negatively affect Rubisco and RCA activity and gene expression, affecting the photosynthetic rate of plants (Bi et al., 2017; Wijewardene et al., 2020). Sudhani and Moreno (2015) identified that GSH can convert Rubisco to an active state by modulating the RCA disulfide bond structure. Some reports have demonstrated that a high GSH/GSSG ratio increases the Rubisco activity and consequently CO_2 assimilation via enhanced thiol and disulfide exchanges (Jiang et al., 2012). The authors' previous study demonstrated that exogenous GSH can improve the CO_2 carboxylation efficiency of tomato seedlings by up-regulating Rubisco and RCA activity as well as *RbcL*, *RbcS* and *RCA* expression under longer periods of salt stress (5, 10 and 15 d) (Liu et al., 2014). The results of the current study demonstrated that exogenous GSH treatment effectively counteracted the inhibitory effects of short-term salt stress (24, 48 and 72 h) on Rubisco activity, RCA activity, and *RbcL*, *RbcS*, and *RCA* expression. However, the beneficial effects of GSH on CO_2 carboxylation efficiency under salt stress were diminished with the addition of exogenous Hb. These results suggested that exogenous GSH improved CO_2 carboxylation and photosynthetic electron transfer efficiency in salt-stressed tomato plants, thereby alleviating photoinhibition caused by NADPH accumulation at the PSI receptor site. Furthermore, NO involvement in the positive regulation of GSH on CO_2 carboxylation efficiency under NaCl stress was investigated. PGK and GAPDH are the main rate-limiting enzymes in the CO_2 reduction phase (Zhang et al., 2011). The activity and gene expression of both directly affected CBC transport efficiency. SBPase (Ding et al., 2016), FBPase (Yu et al., 2020), TK (Bi et al., 2019) and FBA are the key enzymes in the RuBP regeneration stage. The strength of FBPase activity directly affects carbohydrate accumulation and photosynthetic efficiency. SBPase is located at the branching point between the assimilation and regeneration phases of the Calvin cycle, controlling

carbon influx and regeneration. FBA catalyzes the cleavage of FBP into DHAP and G3P. These reactions play a role in plant responses to abiotic adversity such as salt stress (Lu et al., 2012). A reduction in TK activity decreases the efficiency of converting carbon-assimilated metabolites, leading to a decline in the photosynthetic rate of plants. *CsTK* antisense plants inhibit the growth of the capacity to assimilate carbon of *Cucumis sativus* under cold stress (Bi et al., 2019). This study demonstrated that exogenous GSH treatment effectively alleviated the inhibitory effects of NaCl stress on key enzyme activity and gene expression in the Calvin cycle (PGK, GAPDH, SBPase, FBPase, FBA and TK) (Figures 8, 9). Hb application attenuated GSH effects to varying degrees. These results suggested that GSH enhanced carbon assimilation efficiency, relieved feedback inhibition of photosynthetic products, and promoted CBC operation, thereby mitigating the decline in carbon assimilation capacity caused by salt stress. Furthermore, NO was shown to be involved in the regulation of GSH on CO_2 reduction and RuBP regeneration stages under salt stress.

5 Conclusion

In summary, the supplementation of exogenous GSH alleviated photoinhibition and enhanced photosynthetic efficiency in tomato seedlings subjected to NaCl stress. This was achieved through optimizing energy utilization in PSII reaction centers, safeguarding the structure and functionality of photosynthetic reaction centers, enhancing photochemical reactions and energy utilization efficiency, facilitating the operation of the Calvin-Benson Cycle, and alleviating the inhibitory effects of photosynthetic products. Moreover, the application of GSH resulted in an elevation of endogenous NO levels through the induction of the NO synthesis pathway. The presence of Hb attenuated the advantageous impacts of GSH on endogenous NO levels, as well as on the structure and functionality of the photosynthetic apparatus, and the efficiency of carbon assimilation in tomato seedlings under salt stress. These findings validated the role of NO in mediating the beneficial impacts of GSH in ameliorating photosynthesis in tomato seedlings under salt stress.

Data availability statement

The original contributions presented in the study are included in the article/Supplementary Material. Further inquiries can be directed to the corresponding authors.

Author contributions

YC: Conceptualization, Data curation, Methodology, Writing – original draft, Writing – review & editing, Investigation, Visualization, Formal analysis. XC: Writing – original draft, Writing – review & editing, Formal analysis, Investigation. JX: Investigation, Writing – original draft, Writing – review & editing, Formal analysis. XL: Investigation, Writing – original draft, Writing – review & editing. SP: Conceptualization, Writing – original draft, Writing – review & editing. HL: Conceptualization, Funding acquisition, Methodology,

Project administration, Resources, Supervision, Writing – original draft, Writing – review & editing.

Funding

The author(s) declare financial support was received for the research, authorship, and/or publication of this article. This work was supported by the National Natural Science Foundation of China (No. 31860550) and earmarked funds for XJARS (XJARS-07).

Conflict of interest

The authors declare that the research was conducted in the absence of any commercial or financial relationships that could be construed as a potential conflict of interest.

References

- Alamri, S., Kushwaha, B. K., Singh, V. P., Siddiqui, M. H., Al-Amri, A. A., Alsubaie, Q. D., et al. (2021). Ascorbate and glutathione independently alleviate arsenate toxicity in brinjal but both require endogenous nitric oxide. *Physiol. Plant* 173, 276–286. doi: 10.1111/ppl.13411
- Bahmani, R., Kim, D., Na, J., and Hwang, S. (2019). Expression of the tobacco non-symbiotic class 1 hemoglobin gene hb1 reduces cadmium levels by modulating cd transporter expression through decreasing nitric oxide and ROS level in *arabidopsis*. *Front. Plant Sci.* 10. doi: 10.3389/fpls.2019.00201
- Baker, N. R. (2008). Chlorophyll fluorescence: A probe of photosynthesis *in vivo*. *Annu. Rev. Plant Biol.* 59, 89–113. doi: 10.1146/annurev.arplant.59.032607.092759
- Bi, H., Li, F., Wang, H., and Ai, X. (2019). Overexpression of transketolase gene promotes chilling tolerance by increasing the activities of photosynthetic enzymes, alleviating oxidative damage and stabilizing cell structure in *Cucumis sativus* L. *Physiologia plantarum* 167, 502–515. doi: 10.1111/ppl.12903
- Bi, H., Liu, P., Jiang, Z., and Ai, X. (2017). Overexpression of the rubisco activase gene improves growth and low temperature and weak light tolerance in *Cucumis sativus*. *Physiol. Plant* 161, 224–234. doi: 10.1111/ppl.12587
- Chen, X., Zhou, Y., Cong, Y., Zhu, P., Xing, J., Cui, J., et al. (2021). Ascorbic acid-induced photosynthetic adaptability of processing tomatoes to salt stress probed by fast OJIP fluorescence rise. *Front. Plant Sci.* 12. doi: 10.3389/fpls.2021.594400
- Diao, M., Ma, L., Wang, J., Cui, J., Fu, A., and Liu, H. (2014). Selenium promotes the growth and photosynthesis of tomato seedlings under salt stress by enhancing chloroplast antioxidant defense system. *J. Plant Growth Regul.* 33, 671–682. doi: 10.1007/s00344-014-9416-2
- Ding, F., Wang, M., Zhang, S., and Ai, X. (2016). Changes in SBPase activity influence photosynthetic capacity, growth, and tolerance to chilling stress in transgenic tomato plants. *Sci. Rep.* 6, 32741. doi: 10.1038/srep32741
- Fancy, N. N., Bahlmann, A. K., and Loake, G. J. (2017). Nitric oxide function in plant abiotic stress. *Plant Cell Environ.* 40, 462–472. doi: 10.1111/pce.12707
- Fatma, M., Asgher, M., Masood, A., and Khan, N. A. (2014). Excess sulfur supplementation improves photosynthesis and growth in mustard under salt stress through increased production of glutathione. *Environ. Exp. Bot.* 107, 55–63. doi: 10.1016/j.envexpbot.2014.05.008
- Gautam, H., Sehar, Z., Rehman, M. T., Hussain, A., AlAjmi, M. F., and Khan, N. A. (2021). Nitric oxide enhances photosynthetic nitrogen and sulfur-use efficiency and activity of ascorbate-glutathione cycle to reduce high temperature stress-induced oxidative stress in rice (*Oryza sativa* L.). *Plants Biomolecules* 11, 305. doi: 10.3390/biom11020305
- Goodarzi, A., Namdjoyan, S., and Soorki, A. A. (2020). Effects of exogenous melatonin and glutathione on zinc toxicity in safflower (*Carthamus tinctorius* L.) seedlings. *Ecotoxicol. Environ. Saf.* 201, 110853. doi: 10.1016/j.ecoenv.2020.110853
- Guo, Y., Lu, Y., Goltsev, V., Strasser, R. J., Kalaji, H. M., Wang, H., et al. (2020). Comparative effect of tenuazonic acid, diuron, bentazone, dibromothymoquinone and methyl viologen on the kinetics of Chl a fluorescence rise OJIP and the MR₈₂₀ signal. *Plant Physiol. Biochem.* 156, 39–48. doi: 10.1016/j.plaphy.2020.08.044
- Harrison, E. P., Willingham, N. M., Lloyd, J. C., and Raines, C. A. (1998). Reduced sedoheptulose-1,7-bisphosphatase levels in transgenic tobacco lead to decreased photosynthetic capacity and altered carbohydrate accumulation. *Planta* 204, 27–36. doi: 10.1007/s004250050226

Publisher's note

All claims expressed in this article are solely those of the authors and do not necessarily represent those of their affiliated organizations, or those of the publisher, the editors and the reviewers. Any product that may be evaluated in this article, or claim that may be made by its manufacturer, is not guaranteed or endorsed by the publisher.

Supplementary material

The Supplementary Material for this article can be found online at: <https://www.frontiersin.org/articles/10.3389/fpls.2024.1413653/full#supplementary-material>

Hasan, M. K., Liu, C., Wang, F., Ahammed, G. J., Zhou, J., Xu, M.-X., et al. (2016). Glutathione-mediated regulation of nitric oxide, S-nitrosothiol and redox homeostasis confers cadmium tolerance by inducing transcription factors and stress response genes in tomato. *Chemosphere* 161, 536–545. doi: 10.1016/j.chemosphere.2016.07.053

Hu, L., Gao, X., Li, Y., Lyu, J., Xiao, X., Zhang, G., et al. (2023). Nitric oxide induced by ammonium/nitrate ratio ameliorates low-light stress in *brassica pekinensis*: regulation of photosynthesis and root architecture. *Int. J. Mol. Sci.* 24, 7271. doi: 10.3390/ijms24087271

Jensen, E., Clement, R., Maberly, S. C., and Gontero, B. (2017). Regulation of the Calvin - Benson - Bassham cycle in the enigmatic diatoms: biochemical and evolutionary variations on an original theme. *Philos. T R Soc. B* 372, 20160401. doi: 10.1098/rstb.2016.0401

Jiang, Y., Wang, D., and Wen, J. (2012). The independent prokaryotic origins of eukaryotic fructose-1, 6-bisphosphatase and sedoheptulose-1, 7-bisphosphatase and the implications of their origins for the evolution of eukaryotic Calvin cycle. *BMC Evol. Biol.* 12, 208. doi: 10.1186/1471-2148-12-208

Khan, M., Ali, S., Al Azzawi, T. N. I., and Yun, B.-W. (2023). Nitric oxide acts as a key signaling molecule in plant development under stressful conditions. *Int. J. Mol. Sci.* 24, 4782. doi: 10.3390/ijms24054782

Lee, B. R., and Hwang, S. (2015). Over-expression of *NtHb1* encoding a non-symbiotic class 1 hemoglobin of tobacco enhances a tolerance to cadmium by decreasing NO (nitric oxide) and Cd levels in *Nicotiana tabacum*. *Environ. Exp. Bot.* 113, 18–27. doi: 10.1016/j.envexpbot.2015.01.003

Li, H., Chang, J., Chen, H., Wang, Z., Gu, X., Wei, C., et al. (2017). Exogenous melatonin confers salt stress tolerance to watermelon by improving photosynthesis and redox homeostasis. *Front. Plant Sci.* 8. doi: 10.3389/fpls.2017.00295

Li, Z., Geng, W., Tan, M., Ling, Y., Zhang, Y., Zhang, L., et al. (2022b). Differential responses to salt stress in four white clover genotypes associated with root growth, endogenous polyamines metabolism, and sodium/potassium accumulation and transport. *Front. Plant Sci.* 13. doi: 10.3389/fpls.2022.896436

Li, X., Wang, S., Chen, X., Cong, Y., Cui, J., Shi, Q., et al. (2022a). The positive effects of exogenous sodium nitroprusside on the plant growth, photosystem II efficiency and Calvin cycle of tomato seedlings under salt stress. *Sci. Hortic.* 299, 111016. doi: 10.1016/j.scienta.2022.111016

Lilley, R. M., and Walker, D. A. (1974). An improved spectrophotometric assay for ribulosebisphosphate carboxylase. *Biochim. Biophys. Acta* 358, 226–229. doi: 10.1016/0005-2744(74)90274-5

Liu, H., He, X., Xiao, C., Cui, J., Xu, W., and Liu, H. (2014). Effects of exogenous GSH on photosynthetic characteristics and expression of key enzyme genes of CO₂ assimilation in leaves of tomato seedlings under NaCl stress. (In chinese). *Ying Yong Sheng Tai Xue Bao* 25, 2637–2644. doi: 10.13287/j.1001-9332.2014.0210

Livak, K. J., and Schmittgen, T. D. (2001). Analysis of relative gene expression data using real-time quantitative PCR and the 2^{-ΔΔCT} method. *Methods* 25, 402–408. doi: 10.1006/meth.2001.1262

Lu, W., Tang, X., Huo, Y., Xu, R., Qi, S., Huang, J., et al. (2012). Identification and characterization of fructose 1,6-bisphosphate aldolase genes in *Arabidopsis* reveal a gene family with diverse responses to abiotic stresses. *Gene* 503, 65–74. doi: 10.1016/j.gene.2012.04.042

- Mueller-Schuessele, S. J., Wang, R., Guetle, D. D., Romer, J., Rodriguez-Franco, M., Scholz, M., et al. (2020). Chloroplasts require glutathione reductase to balance reactive oxygen species and maintain efficient photosynthesis. *Plant J.* 103, 1140–1154. doi: 10.1111/tpj.14791
- Murchie, E. H., and Niyogi, K. K. (2011). Manipulation of photoprotection to improve plant photosynthesis. *Plant Physiol.* 155, 86–92. doi: 10.1104/pp.110.168831
- Parveen, N., Kandhol, N., Sharma, S., Singh, V. P., Chauhan, D. K., Ludwig-Müller, J., et al. (2023). Auxin crosstalk with reactive oxygen and nitrogen species in plant development and abiotic stress. *Plant Cell Physiol.* 63, 1814–1825. doi: 10.1093/pcp/pcac138
- Sarabi, B., Fresneau, C., Ghaderi, N., Bolandnazar, S., Streb, P., Badeck, F.-W., et al. (2019). Stomatal and non-stomatal limitations are responsible in down-regulation of photosynthesis in melon plants grown under the saline condition: application of carbon isotope discrimination as a reliable proxy. *Plant Physiol. BIOCH* 141, 1–19. doi: 10.1016/j.plaphy.2019.05.010
- Semida, W. M., Abd El-Mageed, T. A., Abdalla, R. M., Hemida, K. A., Howladar, S. M., Leilah, A. A. A., et al. (2021). Sequential antioxidants foliar application can alleviate negative consequences of salinity stress in *vicia faba* L. *Plants Basel* 10, 914. doi: 10.3390/plants10050914
- Shao, R., Wang, K., and Shangguan, Z. (2010). Cytokinin-induced photosynthetic adaptability of *Zea mays* L. to drought stresses associated with nitric oxide signal: Probed by ESR spectroscopy and fast OJIP fluorescence rise. *J. Plant Physiol.* 167, 472–479. doi: 10.1016/j.jplph.2009.10.020
- Shi, C., Yang, F., Liu, Z., Li, Y., Di, X., Wang, J., et al. (2021). Uniform water potential induced by salt, alkali, and drought stresses has different impacts on the seedling of *hordeum jubatum*: from growth, photosynthesis, and chlorophyll fluorescence. *Front. Plant Sci.* 12. doi: 10.3389/fpls.2021.733236
- Simkin, A. J., Lopez-Calcagno, P. E., and Raines, C. A. (2019). Feeding the world: improving photosynthetic efficiency for sustainable crop production. *J. Exp. Bot.* 70, 1119–1140. doi: 10.1093/jxb/ery445
- Sudhani, H. P. K., and Moreno, J. (2015). Control of the ribulose 1,5-bisphosphate carboxylase/oxygenase activity by the chloroplastic glutathione pool. *Arch. Biochem. Biophys.* 567, 30–34. doi: 10.1016/j.abb.2014.12.032
- Timilsina, A., Dong, W., Hasanuzzaman, M., Liu, B., and Hu, C. (2022). Nitrate-nitrite-nitric oxide pathway: A mechanism of hypoxia and anoxia tolerance in plants. *Int. J. Mol. Sci.* 23, 11522. doi: 10.3390/ijms231911522
- Wani, K. I., Naeem, M., Castroverde, C. D. M., Kalaji, H. M., Albaqami, M., and Aftab, T. (2021). Molecular mechanisms of nitric oxide (NO) signaling and reactive oxygen species (ROS) homeostasis during abiotic stresses in plants. *Int. J. Mol. Sci.* 22, 9656. doi: 10.3390/ijms22179656
- Wen, Z., Liu, H., Zhou, Y., Xianjun, C., and Feng, Y. (2018). The involvement of nitric oxide in exogenous glutathione regulates antioxidant defense capacity against salt stress in tomato seedlings (In Chinese). *J. Plant Physiol.* 54, 607–617. doi: 10.13592/j.cnki.pppj.2017.0432
- Wijewardene, I., Mishra, N., Sun, L., Smith, J., Zhu, X., Payton, P., et al. (2020). Improving drought-, salinity-, and heat-tolerance in transgenic plants by co-overexpressing Arabidopsis vacuolar pyrophosphatase gene *AVP1* and Larrea Rubisco activase gene *RCA*. *Plant Sci.* 296, 110499. doi: 10.1016/j.plantsci.2020.110499
- Wu, P., Xiao, C., Cui, J., Hao, B., Zhang, W., Yang, Z., et al. (2021). Nitric oxide and its interaction with hydrogen peroxide enhance plant tolerance to low temperatures by improving the efficiency of the calvin cycle and the ascorbate-glutathione cycle in cucumber seedlings. *J. Plant Growth Regul.* 40, 2390–2408. doi: 10.1007/s00344-020-10242-w
- Xu, J., Wei, Z., Lu, X., Liu, Y., Yu, W., and Li, C. (2023). Involvement of nitric oxide and melatonin enhances cadmium resistance of tomato seedlings through regulation of the ascorbate-glutathione cycle and ROS metabolism. *Int. J. Mol. Sci.* 24, 9526. doi: 10.3390/ijms24119526
- Yang, Z., Wang, X., Cui, J., Liu, H., Cui, H., and Wu, P. (2023). Nitric oxide and glutathione act synergistically to improve PSII activity and PSI electron transfer under chilling stress in cucumber leaves. *J. Plant Growth Regul.* 42, 5558–5573. doi: 10.1007/s00344-023-10936-x
- Yang, Y., Xie, J., Li, J., Zhang, J., Zhang, X., Yao, Y., et al. (2022). Trehalose alleviates salt tolerance by improving photosynthetic performance and maintaining mineral ion homeostasis in tomato plants. *Front. Plant Sci.* 13. doi: 10.3389/fpls.2022.974507
- Yao, M., Ge, W., Zhou, Q., Zhou, X., Luo, M., Zhao, Y., et al. (2021). Exogenous glutathione alleviates chilling injury in postharvest bell pepper by modulating the ascorbate-glutathione (AsA-GSH) cycle. *Food Chem.* 352, 129458. doi: 10.1016/j.foodchem.2021.129458
- Yu, A., Xie, Y., Pan, X., Zhang, H., Cao, P., Su, X., et al. (2020). Photosynthetic phosphoribulokinase structures: enzymatic mechanisms and the redox regulation of the calvin-benson-bassham cycle. *Plant Cell* 32, 1556–1573. doi: 10.1105/tpc.19.00642
- Yuan, Y., Shu, S., Li, S., He, L., Li, H., Du, N., et al. (2014). Effects of exogenous putrescine on chlorophyll fluorescence imaging and heat dissipation capacity in cucumber (*Cucumis sativus* L.) under salt stress. *J. Plant Growth Regul.* 33, 798–808. doi: 10.1007/s00344-014-9427-z
- YuPing, J., Fei, C., YanHong, Z., Xiao-Jian, X., WeiHua, M., Kai, S., et al. (2012). Cellular glutathione redox homeostasis plays an important role in the brassinosteroid-induced increase in CO₂ assimilation in *Cucumis sativus*. *New Phytol.* 194, 932–943. doi: 10.1111/j.1469-8137.2012.04111.x
- Zhang, W., He, X., Chen, X., Han, H., Shen, B., Diao, M., et al. (2023). Exogenous selenium promotes the growth of salt-stressed tomato seedlings by regulating ionic homeostasis, activation energy allocation and CO₂ assimilation. *Front. Plant Sci.* 14. doi: 10.3389/fpls.2023.1206246
- Zhang, X.-H., Rao, X.-L., Shi, H.-T., Li, R.-J., and Lu, Y.-T. (2011). Overexpression of a cytosolic glyceraldehyde-3-phosphate dehydrogenase gene *OsGAPC3* confers salt tolerance in rice. *Plant Cell Tis Org* 107, 1–11. doi: 10.1007/s11240-011-9950-6
- Zhao, H., Tang, Q., Chang, T., Xiao, Y., and Zhu, X.-G. (2021). Why an increase in activity of an enzyme in the Calvin-Benson cycle does not always lead to an increased photosynthetic CO₂ uptake rate?—a theoretical analysis. *silico Plants* 3, diaa009. doi: 10.1093/insilicoplants/diaa009
- Zhou, Y., Diao, M., Cui, J., Chen, X., Wen, Z., Zhang, J., et al. (2018). Exogenous GSH protects tomatoes against salt stress by modulating photosystem II efficiency, absorbed light allocation and H₂O₂-scavenging system in chloroplasts. *J. Integr. Agric.* 17, 2257–2272. doi: 10.1016/S2095-3119(18)62068-4
- Zhou, Y., Wen, Z., Zhang, J., Chen, X., Cui, J., Xu, W., et al. (2017). Exogenous glutathione alleviates salt-induced oxidative stress in tomato seedlings by regulating glutathione metabolism, redox status, and the antioxidant system. *Sci. Hortic.* 220, 90–101. doi: 10.1016/j.scienta.2017.02.021
- Zhu, J.-K. (2016). Abiotic stress signaling and responses in plants. *Cell* 167, 313–324. doi: 10.1016/j.cell.2016.08.029
- Zushi, K., and Matsuzoe, N. (2017). Using of chlorophyll a fluorescence OJIP transients for sensing salt stress in the leaves and fruits of tomato. *Sci. Hortic.* 219, 216–221. doi: 10.1016/j.scienta.2017.03.016